

University of Groningen

Modeling memory effects in activity-driven networks

Zino, Lorenzo; Rizzo, Alessandro; Porfiri, Maurizio

Published in:
SIAM Journal on Applied Dynamical Systems

DOI:
[10.1137/18M1171485](https://doi.org/10.1137/18M1171485)

IMPORTANT NOTE: You are advised to consult the publisher's version (publisher's PDF) if you wish to cite from it. Please check the document version below.

Document Version
Publisher's PDF, also known as Version of record

Publication date:
2018

[Link to publication in University of Groningen/UMCG research database](#)

Citation for published version (APA):
Zino, L., Rizzo, A., & Porfiri, M. (2018). Modeling memory effects in activity-driven networks. *SIAM Journal on Applied Dynamical Systems*, 17(4), 2830-2854. <https://doi.org/10.1137/18M1171485>

Copyright

Other than for strictly personal use, it is not permitted to download or to forward/distribute the text or part of it without the consent of the author(s) and/or copyright holder(s), unless the work is under an open content license (like Creative Commons).

The publication may also be distributed here under the terms of Article 25fa of the Dutch Copyright Act, indicated by the "Taverne" license. More information can be found on the University of Groningen website: <https://www.rug.nl/library/open-access/self-archiving-pure/taverne-amendment>.

Take-down policy

If you believe that this document breaches copyright please contact us providing details, and we will remove access to the work immediately and investigate your claim.

Downloaded from the University of Groningen/UMCG research database (Pure): <http://www.rug.nl/research/portal>. For technical reasons the number of authors shown on this cover page is limited to 10 maximum.

Modeling Memory Effects in Activity-Driven Networks*

Lorenzo Zino[†], Alessandro Rizzo[‡], and Maurizio Porfiri[§]

Abstract. Activity-driven networks (ADNs) have recently emerged as a powerful paradigm to study the temporal evolution of stochastic networked systems. All the information on the time-varying nature of the system is encapsulated into a constant activity parameter, which represents the propensity to generate connections. This formulation has enabled the scientific community to perform effective analytical studies on temporal networks. However, the hypothesis that the whole dynamics of the system is summarized by constant parameters might be excessively restrictive. Empirical studies suggest that activity evolves in time, intertwined with the system evolution, causing burstiness and clustering phenomena. In this paper, we propose a novel model for temporal networks, in which a self-excitement mechanism governs the temporal evolution of the activity, linking it to the evolution of the networked system. We investigate the effect of self-excitement on the epidemic inception by comparing the epidemic threshold of a Susceptible–Infected–Susceptible model in the presence and in the absence of the self-excitement mechanism. Our results suggest that the temporal nature of the activity favors the epidemic inception. Hence, neglecting self-excitement mechanisms might lead to harmful underestimation of the risk of an epidemic outbreak. Extensive numerical simulations are presented to support and extend our analysis, exploring parameter heterogeneities and noise, transient dynamics, and immunization processes. Our results constitute a first, necessary step toward a theory of ADNs that accounts for memory effects in the network evolution.

Key words. Hawkes process, epidemic threshold, self-excitement, SIS model, stochastic differential equation, time-varying network

AMS subject classifications. 37H10, 60H10, 90B15, 92D25

DOI. 10.1137/18M1171485

1. Introduction. Most real-world systems are unceasingly evolving, and social communities are no exception. Empirical studies have shown that the pattern of connections between individuals evolves in time [35, 36, 43, 66, 86], and their heterogeneous propensity to generate

*Received by the editors February 20, 2018; accepted for publication (in revised form) by L. Billings September 25, 2018; published electronically December 11, 2018.

<http://www.siam.org/journals/siads/17-4/M117148.html>

Funding: This work was supported by the National Science Foundation under grant CMMI-1561134, the Army Research Office under grant W911NF-15-1-0267, with Drs. A. Garcia and S. C. Stanton as program managers, by Compagnia di San Paolo, and by the Italian Ministry of Education, Universities and Research under grant Dipartimenti di Eccellenza 2018-2022.

[†]Department of Mathematical Sciences “G. L. Lagrange,” Politecnico di Torino, 10129 Torino, Italy, Department of Mathematics “G. Peano,” Università di Torino, 10123 Torino, Italy, and Department of Mechanical and Aerospace Engineering, Tandon School of Engineering, New York University, Brooklyn, NY 11201 (lorenzo.zino@unito.it, <http://calvino.polito.it/~zino>).

[‡]Department of Electronics and Telecommunications, Politecnico di Torino, 10129 Torino, Italy, and Office of Innovation, Tandon School of Engineering, New York University, Brooklyn, NY 11201 (alessandro.rizzo@polito.it, <http://staff.polito.it/alessandro.rizzo>).

[§]Department of Mechanical and Aerospace Engineering, Tandon School of Engineering, New York University, Brooklyn, NY 11201 (mporfiri@nyu.edu, <http://faculty.poly.edu/~mporfiri>).

connections is subject to burstiness, which yields temporal clusters of connections separated by latency periods [3, 8, 27, 37, 40, 46, 85]. These two dynamics are often intertwined through memory and self-excitement mechanisms, such that the temporal evolution of the system depends on the evolution of the characteristics of the single individuals, and vice versa [87]. Empirical evidence from the analysis of real-world data supports the presence of self-excitement mechanisms in many biological, social, and economical systems [25, 54, 56]. In this vein, the more an individual is active in generating links and connections with others, the more he/she tends to further increase his/her activity in such tasks. Together with other mechanisms, such as “rich get richer” dynamics [64], self-excitement contributes to the emergence of significant phenomena, such as burstiness, temporal clustering of events, and heavy-tailed distributions, as shown in [54, 58, 87].

The temporal evolution of the network of interactions has recently been modeled through activity-driven networks (ADNs) [69]. Early versions of ADNs entail the definition of a time-invariant activity parameter, which represents an individual’s propensity to interact with other individuals. Then, the pattern of connections is dynamically generated according to a probabilistic rule determined by the activity parameter. Epidemics [30, 51, 52, 69, 89, 91], percolation [81], the spread of innovation [76], and opinion dynamics [50] have been extensively analyzed through ADNs, touching on real-world features, such as heterogeneous attractiveness [2, 71], modularity [62], and coupled structures [48]. Alternative approaches to deal with time-varying interactions have been formulated in network models of social behavior, such as adaptive and/or co-evolving networks [29, 33, 38, 79].

Few attempts have been made to account for the temporal evolution of individuals’ characteristics within the ADN paradigm. The reduction of social activity due to illness has been considered in ADN-based epidemic models [59, 74, 75, 90]. However, the mechanisms proposed in these studies are only able to model state-dependent variations and cannot account for burstiness and clustering phenomena. Some efforts have included memory mechanisms on the link formation process, which increases the probability to connect with individuals who have already been contacted in the past [41, 83]. These memory mechanisms elicit the emergence of “strong” recurrent connections, but do not affect individual characteristics, which remain constant throughout the evolution of the network. Finally, significant attempts to tackle burstiness in temporal networks can be found in [34, 42, 85], where dedicated models have been established through a modification of the interevent time distribution. However, both the inclusion of memory [41, 83] and burstiness [34, 42, 85] in these models have a serious drawback. More specifically, the Markov property is lost, thereby hindering analytical tractability.

Here, we address self-excitement mechanisms within an analytically tractable mathematical model for temporal networks that generalizes the standard ADN paradigm. Toward a realistic description of individual self-excitement, we use Hawkes processes [19, 31, 47] to model nodes’ activations, rather than time-homogeneous processes, which are typically used in standard implementations of ADNs [69, 89]. These time-homogeneous processes may not reflect the temporal characteristics of real-world phenomena, as extensively discussed in [68]. Hawkes processes, introduced in the 1970s [31] with a primary application in seismic events [55], have recently become popular in several fields of investigation, encompassing financial events [5, 16, 32], crime [58, 82], civilian deaths in conflicts [49], events in social

media [9, 73, 87], social interactions [25, 56], and animal locomotion [61].

We first study how self-excitement mechanisms dynamically shape the propensity of individuals in establishing connections with their peers in our novel mathematical model. Then, we investigate how the outcome of an epidemic spreading is modified by the introduction of such an individual dynamics. Our approach allows for the analytical computation of the epidemic threshold in the thermodynamic limit, that is, when the number of individuals tends to infinity [44, 45], and reveals that, in our setting, self-excitement dynamics tend to decrease the epidemic threshold, thus favoring the inception of the epidemic process. This result offers a strong motivation for our analysis. In fact, neglecting self-excitement might lead to the underestimation of the risk of the spread of an infectious disease, with harmful consequences for the society.

A wide range of numerical simulations is presented to deepen the understanding of the model. We examine the effect of heterogeneity and noise in the self-excitement mechanism among individuals, the evolution of the epidemic prevalence (also known as epidemic curve) when the disease becomes endemic, and the combined effect of self-excitement and immunization on epidemic spreading. The results of our numerical simulations yield new insights into the epidemic dynamics. For example, in our model we find that heterogeneity translates into an increased variability of the activity rate distribution and, differently from what is observed in the ADN model with memory proposed in [83], immunization seems to further promote the inception of the epidemic in the presence of self-excitement mechanisms.

The rest of the paper is organized as follows. In section 2, we introduce Hawkes processes and analyze their long-run behavior. In section 3, we formalize our generalized ADN-based model that includes self-excitement. Section 4 is devoted to the analytical treatment of the model. In section 5, we present our numerical results. Finally, section 6 summarizes our results and concludes the paper.

2. Hawkes processes. Discrete-event dynamical systems, such as the evolution of temporal networks, can be conveniently modeled by point processes that generate the event occurrences [13]. A point process is represented by its counting process N_t , taking values in the nonnegative integer set \mathbb{N} , which counts the number of occurrences of an event up to time t [7]. Time is treated as a continuous, real variable, taking values in \mathbb{R}^+ , which is the set of nonnegative real numbers, such that $N_0 = 0$. The counting process N_t is characterized by a stochastic law governing the distribution of the interevent times. In this setting, events are assumed to be instantaneous. Poisson processes are the most used point processes in applications [7]. They are characterized by a unique (possibly time-varying) parameter a_t , named *intensity*, such that the probability that an event occurs in the time window between t and $t + \Delta t$ is equal to

$$(2.1) \quad \mathbb{P}[N_{t+\Delta t} - N_t = 1] = \int_t^{t+\Delta t} a_s ds + o(\Delta t).$$

If a_t is constant in time and equal to a , the process is said to be *homogeneous*, the integral in (2.1) is independent of time t , and it reduces to the product $a\Delta t$ [7].

Due to their analytical tractability, homogeneous Poisson processes have often been used in the literature to model the occurrence of instantaneous events in social systems [65, 67, 89].

However, homogeneous Poisson processes may be inadequate to represent point processes underlying real-world social systems, whose intensities are seldom constant in time [8, 68]. Hawkes processes have recently emerged as a powerful modeling tool to address this issue [32]. The rationale for these processes is that the intensity of real-world processes is often influenced by the occurrences of the process itself through two mechanisms: (i) a self-excitement effect, which increases the intensity at each occurrence of the point process; and (ii) a forgetting mechanism, through which the self-excitement effect of previous occurrences tends to vanish in time.

Formally, a Hawkes process is a nonhomogeneous Poisson point process, whose counting process N_t follows (2.1) with a time-varying intensity a_t that is ruled by the stochastic differential equation (SDE) [63]

$$(2.2) \quad da_t = \gamma(\hat{a} - a_t)dt + JdN_t.$$

Three parameters define Hawkes processes: (i) the *jump* $J \geq 0$, which measures the magnitude of the intensity increase due to the self-excitement effect; (ii) the *forgetting rate* $\gamma > 0$, which determines the velocity of the forgetting process; and (iii) the *background activity* $\hat{a} > 0$, which poses a lower barrier for the forgetting mechanism and represents the intensity of the process in the absence of self-excitement. In our framework, we set the jump J as a constant. In a general formulation of Hawkes processes [16, 17, 31], the jump may be set as a random variable (RV), such that each variation in the intensity would be obtained as a different realization of the RV.

Equation (2.2) can be integrated by applying Ito's lemma to $a_t e^{\gamma t}$, obtaining [16]

$$(2.3) \quad a_t = \hat{a} + (a_0 - \hat{a})e^{-\gamma t} + J \int_0^t e^{-\gamma(t-s)} dN_s,$$

where $a_0 \geq 0$ is the initial condition for the intensity and the computation of the integral requires the concurrent solution of (2.2).

Hawkes processes (N_t, a_t) satisfy the Markov property [7], since the value of the intensity a_t alone encapsulates all the past history of the process up to time t . In fact, given the process state at time t , its evolution at any time $s > t$ only depends on a_t , which, in turn, is governed by (2.2) and only depends on the value of the process at time t .

Remark 2.1. For small time steps Δt , a discrete-time approximation of (2.3) is

$$(2.4) \quad a_{t+\Delta t} \approx a_t e^{-\gamma \Delta t} + \hat{a}(1 - e^{-\gamma \Delta t}) + J\xi_t,$$

and the corresponding evolution of the Hawkes process is

$$(2.5) \quad N_{t+\Delta t} \approx N_t + \xi_t,$$

where ξ_t is a Poisson-distributed RV with intensity $a_t \Delta t$. Also, when $\Delta t \rightarrow 0$, the probability that ξ_t assumes values larger than 1 becomes negligible [7]. Therefore, the Poisson RV ξ_t can be approximated by a Bernoulli RV with parameter $a_t \Delta t$ [7]. This discrete-time approximation enables the implementation of fast numerical simulations.

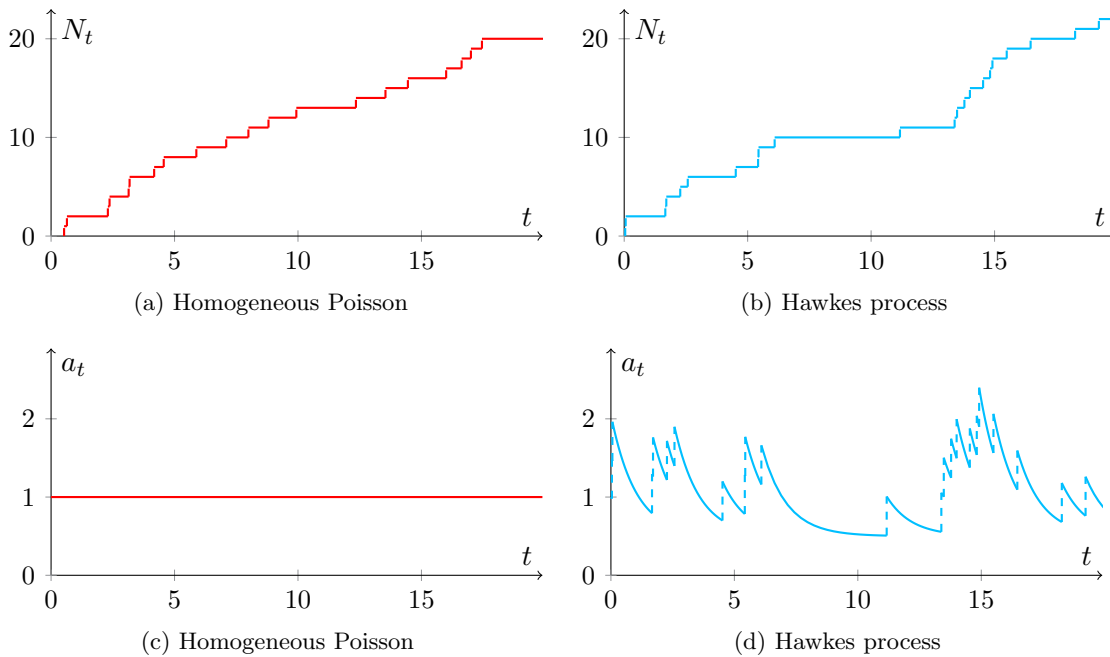


Figure 1. Comparison between sample path (a) and intensity (c) of a homogeneous Poisson process with intensity 1, and the corresponding quantities (b), (d) in a Hawkes process with $a_0 = 1$, $\hat{a} = 0.5$, $J = 0.4$, and $\gamma = 0.8$. The activity of the Hawkes process presents burstiness, and its events tend to cluster close to the intensity peaks.

Figure 1 compares a homogeneous Poisson process with a Hawkes process, highlighting that the events of a Hawkes process tend to occur in clusters. This feature is consistent with the phenomenon of burstiness in social behavior [8, 27, 46]. An alternative strategy to include burstiness into network models consists of the use of non-Poisson renewal processes, which can represent any desired interevent distribution [34, 42]. However, these models do not share the Markov property, thereby challenging their analytical treatment. The Markov property enables the proof of the following results concerning the first two moments of the intensity of Hawkes processes, which will be useful in what follows.

Lemma 2.2. Let (N_t, a_t) be a Hawkes process such that $J/\gamma < 1$. Then, a_t converges to an asymptotic invariant distribution a_∞ such that

$$(2.6) \quad \mathbb{E}[a_\infty] = \frac{\hat{a}}{1 - \frac{J}{\gamma}} \quad \text{and} \quad \mathbb{E}[a_\infty^2] = \frac{\hat{a}^2}{\left(1 - \frac{J}{\gamma}\right)^2} + \frac{J^2 \hat{a}}{2\gamma \left(1 - \frac{J}{\gamma}\right)^2}.$$

Proof. Following [16], we can describe the evolution of $\mathbb{E}[a_t]$ and $\mathbb{E}[a_t^2]$ through the following pair of ordinary differential equations (ODEs):

$$(2.7a) \quad \frac{d\mathbb{E}[a_t]}{dt} = \gamma \hat{a} + (J - \gamma)\mathbb{E}[a_t],$$

$$(2.7b) \quad \frac{d\mathbb{E}[a_t^2]}{dt} = (J^2 + 2\gamma\hat{a})\mathbb{E}[a_t] + 2(J - \gamma)\mathbb{E}[a_t^2].$$

The derivation of these ODEs is performed in a probabilistic framework. The Markov property of the Hawkes process allows for the application of Dynkin’s formula [63], that is,

$$(2.8) \quad \mathbb{E}[a_t^h] = a^h(0) + \mathbb{E} \left[\int_0^t \mathcal{L} [a_s^h] ds \right],$$

where the operator $\mathcal{L}[\cdot]$ is the infinitesimal generator of the stochastic process [63]. For the case of Hawkes processes, $\mathcal{L}[a_s^h]$ has been explicitly computed in [16]. Finally, the Fubini–Tonelli theorem allows for swapping the order of expectation and integration operators, and differentiation with respect to variable t yields (2.7a) and (2.7b). Further details can be found in [16, 19].

The integration of (2.7a) under the condition $J < \gamma$ is straightforward [17], yielding

$$(2.9) \quad \mathbb{E}[a_t] = \frac{\hat{a}}{1 - \frac{J}{\gamma}} + \left(a(0) - \frac{\hat{a}}{1 - \frac{J}{\gamma}} \right) e^{-(\gamma-J)t},$$

and, similarly, the integration of (2.7b) for $J < \gamma$ gives

$$(2.10) \quad \begin{aligned} \mathbb{E}[a_t^2] &= \frac{\hat{a}^2}{\left(1 - \frac{J}{\gamma}\right)^2} + \frac{J^2\hat{a}}{2\gamma\left(1 - \frac{J}{\gamma}\right)^2} \\ &+ \left[\left(a(0) - \frac{\hat{a}}{1 - \frac{J}{\gamma}} \right)^2 - \frac{J^2\left(2a(0) - \frac{\hat{a}}{1 - \frac{J}{\gamma}} \right)}{2\gamma\left(1 - \frac{J}{\gamma}\right)} \right] e^{-2(\gamma-J)t} \\ &+ \left[2\left(a(0) - \frac{\hat{a}}{1 - \frac{J}{\gamma}} \right) \frac{\hat{a}}{\left(1 - \frac{J}{\gamma}\right)} + \frac{J^2\left(a(0) - \frac{\hat{a}}{1 - \frac{J}{\gamma}} \right)}{\gamma\left(1 - \frac{J}{\gamma}\right)} \right] e^{-(\gamma-J)t}. \end{aligned}$$

The proof of the asymptotic results is completed by computing the limit of (2.9) and (2.10) for $t \rightarrow \infty$.

For the purpose of this work, the convergence of the first two moments of the intensity is sufficient to perform further computations. However, for the sake of completeness, we remark that for $J/\gamma < 1$, the intensity a_t weakly converges to a stationary distribution a_∞ , whose first two moments are those detailed in (2.6). Then, a phase transition occurs at $J = \gamma$, separating a subcritical (stable) regime and a supercritical (unstable) one. In the supercritical regime, the intensity a_t does not weakly converge to any stationary distribution. Under our assumptions, the system is always in the stable regime. For further details, see [12, 17]. ■

Remark 2.3. From Lemma 2.2, we observe that the behavior of the quantities of interest, i.e., the first two moments of the intensity, is subject to the following set of considerations.

- The ratio $J/\gamma \in [0, 1)$ controls the increase in the asymptotic average intensity with respect to the background intensity: when the ratio is equal to 0, the two averages coincide; as the ratio tends to 1, the asymptotic average intensity grows.

- The ratio $J^2/\gamma \in \mathbb{R}^+$ regulates the asymptotic variability of the intensity: the larger the ratio, the broader the asymptotic distribution of the intensity.
- The difference $\gamma - J$ determines the speed of convergence to the asymptotic quantities. The larger this difference, the faster the convergence is. Slow convergence occurs if either (i) J and γ are both close to 0, or (ii) J and γ are large but very close to each other. However, (i) is the case where the self-excitement is negligible and (ii) is the extreme case close to the phase transition where the asymptotic average intensity blows up. Therefore, under our assumptions on J and γ , if self-excitement is nonnegligible, fast convergence can always be assumed, so that the quantities always converge exponentially to their corresponding asymptotic values.

In the rest of this work, we associate a Hawkes process with each individual of a population, in order to model his/her activation patterns. To enhance readability, we will denote the time variable of the Hawkes processes in parentheses, whereas subscripts will be used to refer to individual Hawkes processes. Therefore, the values of the counting process and its intensity at time t for the Hawkes process associated with individual v will be denoted by $N_v(t)$ and $a_v(t)$, respectively.

3. ADN+HP model. Here, we formalize our model by including into the ADN paradigm self-excitement mechanisms, defined through Hawkes processes. We name the resulting model ADN+HP.

In the literature, ADNs have been defined according to two different formalisms: the original formulation comprises a discrete-time process [69], while a continuous-time counterpart has been proposed in [89, 90]. In [89], it has been proved that the two formulations coincide in the limit when the time-step of the discrete-time model tends to 0. Moreover, a technique to rescale the parameters from one model to the other has been presented and discussed therein. The continuous-time framework has the advantages of relying on fewer parameters and being independent of the confounding factors due to the selection of the discrete time-step [72], ultimately leading to a model that is amenable to analytical treatment.

The considerations above and the original definition of Hawkes processes in continuous time prompt us to formalize our model using continuous-time ADNs. However, it is straightforward to move to the discrete-time formalism when needed, for example during numerical simulations [89].

We consider a population of n individuals, each one identified by a node on a temporal network $\mathcal{G} = (\mathcal{V}, \mathcal{E}(t))$, where $\mathcal{V} = \{1, \dots, n\}$ is the node set and $\mathcal{E}(t)$ is a time-varying link set. Node v activates according to a Hawkes process $(N_v(t), a_v(t))$, and each process is independent of the others. Specifically, $a_v(t)$ is governed by the following SDE:

$$(3.1) \quad da_v(t) = \gamma_v (\hat{a}_v - a_v(t)) dt + J_v dN_v(t), \quad v \in \mathcal{V},$$

with initial condition $a_v(0) > 0$.

We summarize the algorithm to generate temporal networks according to a continuous-time ADN+HP model as follows:

1. At time $t = 0$, we set $\mathcal{E}(t) = \emptyset$, and, for each node $v \in \mathcal{V}$, an independent Hawkes process $(N_v(t), a_v(t))$ is initialized with given initial intensity $a_v(0)$.

2. If the Hawkes process associated with node v has a jump at time t , then node v activates.
3. Once node v activates, then it generates an instantaneous undirected link by connecting to a node in $w \in \mathcal{V}$ uniformly chosen at random. The undirected link $\{v, w\}$ is added to $\mathcal{E}(t)$.
4. The instantaneous link is immediately removed from the link set, and the procedure reverts to step 2.

The mechanism described above creates ephemeral connections through which pairs of individuals can establish spreading-like dynamical processes, such as epidemic spreading, exchange of information, payments, etc., according to the specific spreading model adopted. In this formulation, self-loops may be present, such that a node is allowed to create a connection with itself. A model without self-loops can be obtained by modifying step 3 of the algorithm above by imposing that the node w is chosen from $\mathcal{V} \setminus \{v\}$. In the specific applications discussed in this paper and in the thermodynamic limit of large-scale populations, the presence of self-loops has a negligible effect on the overall evolution. However, in other applications and/or in different settings, self-loops might not be dismissed. Hence, the possibility of generating time-varying networks either with or without self-loops could be of interest; see, e.g., [24].

Hence, the ADN+HP model is defined by the following parameters:

- the node set $\mathcal{V} = \{1, \dots, n\}$;
- the n -dimensional jump vector $J \geq 0$ (entrywise), whose v th component J_v represents the activity increase after an activation of node v ;
- the n -dimensional forgetting rate vector $\gamma > 0$ (entrywise), whose v th component γ_v represents the velocity with which individual v forgets its excitement due to its previous activations;
- the n -dimensional initial activity rate vector $a(0) > 0$ (entrywise), whose v th component $a_v(0)$ represents the initial activity rate of node v ; and
- the n -dimensional background activity rate vector $\hat{a} > 0$ (entrywise), whose v th component \hat{a}_v represents the background activity rate of node v .

Remark 3.1. If $J = 0$ and $a(0) = \hat{a}$, we retrieve the standard ADN model [69, 89, 90]. Therefore, the ADN+HP model encompasses and generalizes the standard ADN model.

Remark 3.2. Real-world features that have been successfully included within the standard ADN framework can be readily included in the proposed ADN+HP model. These features encompass behavioral changes due to node state [74], heterogeneous propensity of nodes to attract connections [2, 71], modular structure [62], and interactions involving more than two individuals [70]. Furthermore, the addition of memory mechanisms related to the emergence of “strong” recurrent connections [41, 83] is straightforward. Communication and reaction delays can be also included, similarly as in [80].

4. Analytical study of ADN+HP. Here, we analyze the ADN+HP model in the thermodynamic limit, i.e., for $n \rightarrow \infty$ and assuming that the model parameters, if they depend on n , then converge uniformly to finite quantities [44, 45]. Specifically, we study the evolution of the activity rate distribution and its effect on the epidemic threshold of a Susceptible–Infected–Susceptible (SIS) model [28]. This analysis offers an example where the self-excitement mech-

anism influences the evolution of the overall network dynamics, thereby emphasizing the necessity of including self-excitement mechanisms in realistic mathematical models of temporal networks.

The interest in the study of epidemic models is not limited to the epidemiological field. In fact, epidemic-like models find several applications in various areas of research that deal with spreading processes [66]. For instance, the inclusion of social phenomena in epidemic-like models can serve to study some aspects of the spread of innovation [23, 76], opinions [53], and false news [84] in social networks, or to predict and control the spread of mutant species in geographical networks [88].

In our analysis, we hypothesize that self-excitement causes nonnegligible jumps (i.e., $J_v > 0 \forall v \in \mathcal{V}$) and that the involved Hawkes processes are in the subcritical regime (i.e., $J_v < \gamma_v \forall v \in \mathcal{V}$). Under these premises, following Remark 2.3, the moments of the intensity of the Hawkes processes rapidly converge to their asymptotic values, according to Lemma 2.2. Toward an analytical treatment of the problem, we also assume that self-excitement and forgetting mechanisms act homogeneously on the whole population. More formally, all the nodes activate according to Hawkes processes with the same jump and forgetting rate, i.e., $J_v = J$ and $\gamma_v = \gamma \forall v \in \mathcal{V}$, and, possibly, different initial and background activity rates $a_v(0)$ and \hat{a}_v . The heterogeneity among individuals is treated through the initial and background activity rates, thereby yielding $2n$ free parameters to calibrate the model and fit real-world parameters. The effect of further heterogeneity factors is numerically analyzed in subsection 5.1.

4.1. Evolution of the activity rate distribution. We investigate the effect of self-excitement in the evolution of the activity rate distribution in ADNs+HP. Specifically, we show that the self-excitement mechanism produces broader activity rate distributions than the distribution of the background activity rates.

To study the evolution of the activity rate distribution, we define its moments as

$$(4.1) \quad M_{a^i(t)} := \frac{1}{n} \sum_{v \in \mathcal{V}} a_v^i(t)$$

for $i \geq 1$. In general, given an n -dimensional vector x , we define M_x as its statistical mean. We assert the following lemma.

Lemma 4.1. *Consider n nodes connected through a temporal network evolving according to an ADN+HP with initial activity rate vector $a(0)$ and background activity rate vector \hat{a} . Then, in the thermodynamic limit, the following equalities hold almost surely:*

$$(4.2a) \quad \lim_{t \rightarrow \infty} M_{a(t)} = \frac{M_{\hat{a}}}{1 - \frac{J}{\gamma}},$$

$$(4.2b) \quad \lim_{t \rightarrow \infty} M_{a^2(t)} = \frac{M_{\hat{a}^2}}{\left(1 - \frac{J}{\gamma}\right)^2} + \frac{J^2 M_{\hat{a}}}{2\gamma \left(1 - \frac{J}{\gamma}\right)^2}.$$

Proof. In the thermodynamic limit, under the hypothesis $J < \gamma$, the Kolmogorov strong

law of large numbers [15] implies that, almost surely,

$$(4.3) \quad M_{a^i(t)} = \frac{1}{n} \sum_{v \in \mathcal{V}} a_v^i(t) = \frac{1}{n} \sum_{v \in \mathcal{V}} \mathbb{E}[a_v^i(t)] = M_{\mathbb{E}[a^i(t)]}.$$

Using Lemma 2.2, and specifically (2.9), we write

$$(4.4) \quad M_{a(t)} = \frac{M_{\hat{a}}}{1 - \frac{J}{\gamma}} + \left(M_{a(0)} - M_{a(0)} \frac{M_{\hat{a}}}{1 - \frac{J}{\gamma}} \right) e^{-(\gamma-J)t}.$$

Then, using (2.10), we obtain

$$(4.5) \quad \begin{aligned} M_{a^2(t)} = & \frac{M_{\hat{a}^2}}{\left(1 - \frac{J}{\gamma}\right)^2} + \frac{J^2 M_{\hat{a}}}{2\gamma \left(1 - \frac{J}{\gamma}\right)^2} + M_{a^2(0)} e^{-2(\gamma-J)t} \\ & + \left[\frac{M_{\hat{a}^2}}{\left(1 - \frac{J}{\gamma}\right)^2} - \frac{2M_{\hat{a}a(0)}}{1 - \frac{J}{\gamma}} - \frac{J^2 M_{a(0)}}{\gamma \left(1 - \frac{J}{\gamma}\right)} + \frac{J^2 M_{\hat{a}}}{2\gamma \left(1 - \frac{J}{\gamma}\right)^2} \right] e^{-2(\gamma-J)t} \\ & + \left[2 \frac{M_{a(0)\hat{a}}}{\left(1 - \frac{J}{\gamma}\right)} - \frac{M_{\hat{a}^2}}{\left(1 - \frac{J}{\gamma}\right)} + \frac{J^2 M_{a(0)}}{\gamma \left(1 - \frac{J}{\gamma}\right)} - \frac{J^2 M_{\hat{a}}}{\gamma \left(1 - \frac{J}{\gamma}\right)^2} \right] e^{-(\gamma-J)t}. \end{aligned}$$

The computation of the limit for $t \rightarrow \infty$ of (4.4) and (4.5) yields the claim. ■

While the effect of the initial distribution vanishes exponentially fast in time, the asymptotic distribution of the activity rates is influenced by the background activity and by the two parameters of the Hawkes process J and γ . The effect of self-excitement resides in the increase of the dispersion of the activity rates with respect to the background activity rate distribution. This feature is typically measured through the coefficient of variation (also known as the relative standard deviation), which is the ratio between the standard deviation and the mean [59],

$$(4.6) \quad c_V[a] := \frac{\sqrt{M_{a^2} - M_a^2}}{M_a} \longrightarrow \sqrt{c_V^2[\hat{a}] + \frac{J^2}{2\gamma M_{\hat{a}}}}.$$

From (4.6), we note that the asymptotic distribution of the activity rates of an ADN+HP process consistently exhibits a more increased dispersion than the background distribution. Moreover, (4.6) highlights the effect of the model parameters. Large values of the jump J tend to drive the activity rates to a broader distribution. On the other hand, an increase in the forgetting rate γ and/or in the mean background activity $M_{\hat{a}}$ yields a narrower distribution.

Figure 2 illustrates an instance of the evolution of the activity rate distribution in an ADN+HP, supporting our analytical findings. For the case presented therein, we start from a homogeneous initial configuration (coinciding with the background one), where all the nodes have the same activity rate $a_v(0) = 0.5$. Then, self-excitement tends to promote the variability in the activity rate distribution of the system, producing a broader asymptotic distribution.

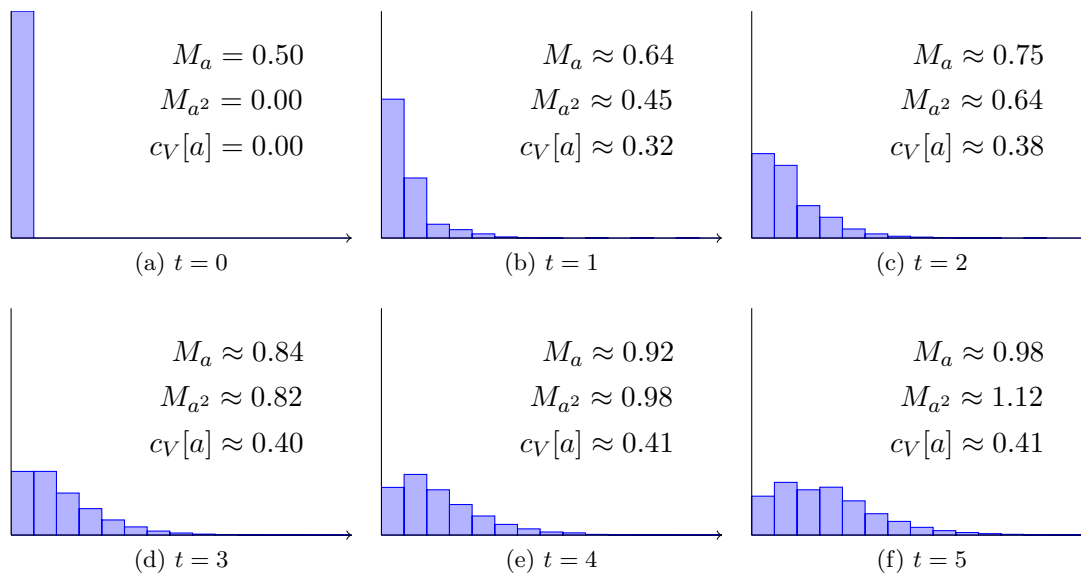


Figure 2. Simulation of the evolution of the activity rate distribution for an ADN+HP model with $n = 100,000$ nodes, starting from a homogeneous initial condition $a(0) = 0.5$, which also coincides with the background activity rate. Model parameters are $J = 0.3$ and $\gamma = 0.5$. From simulations, we observe that the distribution becomes broader and more disperse, which supports our theoretical predictions.

From Lemma 4.1, we analytically compute $M_{a(\infty)} = 1.25$, $M_{a^2(\infty)} = 1.875$, and $c_V[a(\infty)] \approx 0.4472$. These results are consistent with our numerical simulations, where at $t = 200$ we determine $M_{a(200)} \approx 1.2514$, $M_{a^2(200)} \approx 1.8706$, and $c_V[a(200)] \approx 0.441$.

The results in Lemma 4.1 hold true only in the thermodynamic limit $n \rightarrow \infty$. However, the numerical simulations in Figure 3 suggest that the asymptotic values of the moments of the activity rate distribution and their corresponding rates of convergence in the thermodynamic limit are valid approximations for relatively small population sizes. Specifically, the accuracy of the approximations is within 2% for $n > 1000$.

4.2. Epidemic threshold for the SIS epidemic model. We investigate the role of self-excitement on the inception of an epidemic outbreak. In particular, we focus on the analytical computation of the epidemic threshold of an SIS epidemic process.

As we embed an SIS epidemic model in the network, a variety of modeling choices are available, depending on the specific properties of the network and on the underlying SIS mechanisms [60]. Consistently with [89], we define an SIS model on an ADN+HP as follows. Each node $v \in \mathcal{V}$ represents an individual of a population and is given a binary state $Y_v(t) \in \{0, 1\}$ to describe whether individual v at time t is susceptible to the epidemic ($Y_v(t) = 0$) or infected ($Y_v(t) = 1$). The state of the nodes is updated as the dynamics evolve according to two competing mechanisms:

- *Spreading.* When a link is generated by the ADN+HP mechanism, an epidemic can spread through it. Specifically, if the undirected link (v, w) is generated, $Y_v(t) = 0$, and $Y_w(t) = 1$, then v contracts the infection and instantaneously changes its state to

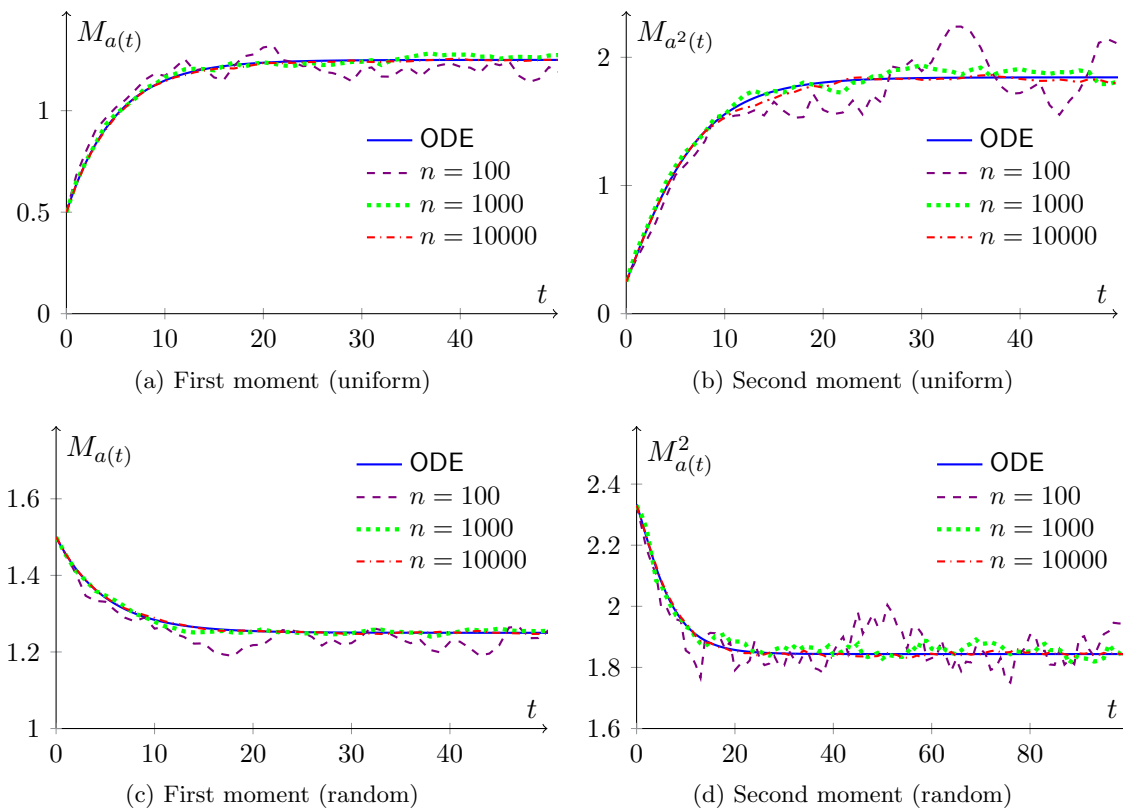


Figure 3. Convergence of the first two moments of the activity rate distribution for an ADN+HP model with increasing numbers of nodes, $n = 100$ (violet dashed), $n = 1000$ (green dotted), and $n = 10,000$ (red dash-dotted), compared with analytical predictions in the asymptotic limit (solid blue), with homogeneous background activity rate $\hat{a} = 0.5$, starting from (a)–(b) a uniform initial condition $a(0) = \hat{a}$, and (c)–(d) a heterogeneous initial condition, distributed uniformly at random in $[1, 2]$. Model parameters are $J = 0.3$ and $\gamma = 0.5$.

1 with a fixed probability $\lambda \in [0, 1]$.

- *Recovery.* Infected nodes recover according to independent homogeneous Poisson processes with rate $\mu > 0$, updating their state from 1 to 0 and becoming susceptible to the epidemic again.

This SIS model exhibits a phase transition between two regimes: one where the epidemic quickly extinguishes, and another where the disease spreads over the population, becoming endemic [6]. The phase transition between these two regimes occurs when passing a specific value of the ratio between the two model parameters $\sigma = \lambda/\mu$. This value is called the epidemic threshold and depends on specific properties of the network of interactions among the individuals of the population [65, 67], degree-correlations [10], structures [22], and seasonality [4]. The precise definition of the two regimes changes according to the modeling choices. In the thermodynamic limit considered in this paper, the *fast extinction regime* is characterized by trajectories that converge to the disease-free equilibrium, while in the *endemic regime*, trajectories with an initial condition different from the disease-free equilibrium do not converge

to it. Other definitions of the two regimes involving the time to extinction can be adopted when studying finite-size populations [21].

The evolution of the system (i.e., the dynamics of the health state of each individual) is governed by an n -dimensional Markov process on the state space $\{0, 1\}^n$, whose size grows exponentially with n , challenging its direct analysis for large-scale systems. Hence, the problem is often solved by studying a continuous relaxation of the dynamics, whose analysis is exact in the thermodynamic limit. Specifically, we compute the epidemic threshold by studying the local linear stability of the origin for the following system of ODEs:

$$(4.7) \quad \dot{y}_v := \frac{d}{dt} \mathbb{E}[Y_v] = -\mu y_v + (1 - y_v) \left(a_v(t) \frac{1}{n} \sum_{w \in \mathcal{V}} y_w + \frac{1}{n} \sum_{w \in \mathcal{V}} a_w(t) y_w \right), \quad v \in \mathcal{V}.$$

System (4.7) models the evolution of the probability of each individual of being infected, rather than the evolution of his/her health state [44, 45, 57, 90].

The analysis of (4.7) is not trivial, due to the presence of the time-varying parameter $a_v(t)$ governed by the SDEs in (3.1). However, in the thermodynamic limit, the analysis can be carried out by means of the law of large numbers and leveraging the asymptotic results for Hawkes processes proved in Lemma 4.1. The following theorem summarizes our results.

Theorem 4.2. *Consider an SIS epidemic model on an ADN+HP. Then, if $J < \gamma$, the epidemic threshold is*

$$(4.8) \quad \sigma_{HP} = \frac{1 - \frac{J}{\gamma}}{M_{\hat{a}} + \sqrt{M_{\hat{a}}^2 + \frac{J^2}{2\gamma} M_{\hat{a}}}}.$$

Specifically, for $\sigma < \sigma_{HP}$, the system is in the fast extinction regime and the epidemic reaches the disease-free equilibrium. On the contrary, for $\sigma > \sigma_{HP}$, the system is in the endemic regime and the epidemic spreads over the population.

Proof. In order to study the linear stability of the origin of the system (4.7), we define a reparametrization of the system through the following macroscopic variables:

$$(4.9) \quad x_i(t) = \frac{1}{n} \sum_{v \in \mathcal{V}} a_v^{i-1}(t) y_v(t),$$

for $i \in \mathbb{Z}^+$, which is the set of positive integer numbers. The first two macroscopic variables have a straightforward physical interpretation. Quantity x_1 counts the fraction of overall infected individuals, while x_2 measures the arithmetic average of the activity rates of infected individuals.

We note that $a_v(t) > 0$ for any $t \geq 0$, since $\hat{a}_v > 0$ and $a_v(0) > 0$. Therefore, the origin in (4.7) coincides with the one in the system of macroscopic variables. In addition, this origin is an asymptotically stable equilibrium of (4.7) if and only if it is asymptotically stable for (4.10a). We also notice that the condition $x_1 = 0$ implies that all the macroscopic variables $x_j = 0$, for any $j \geq 1$. Hence, it is sufficient to study the linear stability of $x_1 = 0$ to ensure the stability of the origin. Following [89] and neglecting second-order terms (which do

not influence the stability of the origin), the evolution of the first two macroscopic variables about the origin is governed by the following ODEs:

$$(4.10a) \quad \dot{x}_1 = (\lambda M_{a(t)} - \mu)x_1 + \lambda x_2,$$

$$(4.10b) \quad \dot{x}_2 = \lambda M_{a^2(t)}x_1 + (\lambda M_{a(t)} - \mu)x_2,$$

coupled with the $2n$ equations in (2.7a) and (2.7b) for the evolution of $\mathbb{E}[a_v]$ and $\mathbb{E}[a_v^2]$, $v \in \mathcal{V}$. These equations determine the evolution of $M_{a(t)}$ and $M_{a^2(t)}$, shown in (4.4) and (4.5).

Hence, we linearize (4.10a) and (4.10b) about the origin, and the $2n$ equations for $\mathbb{E}[a_v]$ and $\mathbb{E}[a_v^2]$ about the (unique stable) equilibrium computed in Lemma 2.2. The obtained linearized system is block-triangular, since the blocks corresponding to the equations derived from (2.7a) and (2.7b) are independent of the macroscopic variables. The stability of these blocks has already been shown in Lemma 2.2. Hence, the stability of the origin is driven by the 2×2 block related to the variables x_1 and x_2 , i.e.,

$$(4.11) \quad J = \begin{bmatrix} -\mu + \lambda \frac{M_a}{1 - \frac{J}{\lambda}} & \lambda \\ \lambda \left(\frac{M_{\hat{a}^2}}{\left(1 - \frac{J}{\gamma}\right)^2} + \frac{J^2 M_{\hat{a}}}{2\gamma \left(1 - \frac{J}{\gamma}\right)^2} \right) & -\mu + \lambda \frac{M_a}{1 - \frac{J}{\lambda}} \end{bmatrix}.$$

The largest eigenvalue of J is equal to

$$(4.12) \quad x = -\mu + \lambda \left[\frac{M_a}{1 - \frac{J}{\lambda}} + \sqrt{\frac{M_{\hat{a}^2}}{\left(1 - \frac{J}{\gamma}\right)^2} + \frac{J^2 M_{\hat{a}}}{2\gamma \left(1 - \frac{J}{\gamma}\right)^2}} \right].$$

This quantity is negative if

$$(4.13) \quad \frac{\lambda}{\mu} < \frac{1 - \frac{J}{\lambda}}{M_{\hat{a}} + \sqrt{M_{\hat{a}^2} + \frac{J^2}{2\gamma} M_{\hat{a}}}},$$

which provides the linear stability condition for the origin.

Before concluding the proof, we remark that this approach cannot fully determine the evolution of the system, since second-order terms cannot be neglected when the system trajectories are away from the origin. Following [89], specific ODEs for the evolution of the macroscopic variables x_j with $j \geq 3$ should be considered. ■

Remark 4.3. In the absence of self-excitement (i.e., $J = 0$), the epidemic threshold for the SIS model in (4.8) coincides with the one found for ADNs in their original formulation [69].

We conclude this section by comparing the epidemic threshold determined in Theorem 4.2 with the threshold for ADNs with time-invariant activity rates that can be found in [69, 89]. This comparison allows for an improved understanding of the effect of self-excitement on the network propensity to the inception of an outbreak. To perform a fair comparison, we set the parameters of the two models such that the two activity rate distributions are consistent, in the sense that each node $i \in \mathcal{V}$ has the same expected activity rate in the two models. Specifically, we compare the SIS model defined above on

1. an ADN+HP with parameters J, γ , and \hat{a} and initial activity rate distribution $a(0)$ coinciding (entrywise) with the expected asymptotic activity rate distribution, that is,

$$(4.14) \quad a_v(0) = \mathbb{E}[a_v(\infty)] = \frac{\hat{a}_v}{1 - J/\gamma}, \quad v \in \mathcal{V}; \quad \text{and}$$

2. a (continuous-time) ADN [89] with time-invariant activity rates $b_v = a_v(0) \forall v \in \mathcal{V}$, equal (entrywise) to the initial and the expected asymptotic values of the ADN+HP model.

From here on, we will refer to two temporal network models with these characteristics as an ADN+HP and its *corresponding* ADN *with time-invariant rates* (or *standard* ADN).

Remark 4.4. By way of construction, the ADN+HP and its corresponding ADN with time-invariant rates are such that, for any node $v \in \mathcal{V}$ and any time $t \in \mathbb{R}^+$, the expected activity rate in the ADN+HP model coincides with the time-invariant activity rate of the same node for the standard ADN.

The epidemic threshold of the SIS model for the ADN+HP is denoted by σ_{HP} , while σ_{ADN} is the one of the corresponding standard ADN. According to [Theorem 4.2](#), their ratio is

$$(4.15) \quad \frac{\sigma_{HP}}{\sigma_{ADN}} = \frac{M_{\hat{a}} + \sqrt{M_{\hat{a}}^2}}{M_{\hat{a}} + \sqrt{M_{\hat{a}}^2 + \frac{J^2}{2\gamma} M_{\hat{a}}}} < 1.$$

Thus, the ADN+HP has a higher propensity toward the inception of epidemic outbreaks than the corresponding standard ADN. From (4.15), we can explicitly quantify this increased propensity as a function of the model parameters. Specifically, while the epidemic threshold has a nontrivial dependence on the background activity rate distribution through its first two moments, the dependence on the self-excitement mechanism is clear and strictly related to the ratio J^2/γ . The larger this ratio, the more prone the system is to the inception of epidemic outbreaks. [Figure 4](#) illustrates this behavior for two significant cases of background activity rate distributions: power-law and homogeneous.

An increase in the network propensity toward the inception of the SIS epidemic has already been documented through numerical simulations that account for memory in the process of link generation [41, 83]. For homogeneous self-excitement parameters and under reasonable assumptions, we have analytically demonstrated this phenomenon. We have been successful in explicitly quantifying the increase of the network propensity to the inception of epidemics as a function of model parameters.

Based on the results on the epidemic threshold discussed above, we stress the importance of including self-excitement into the network dynamics through an explanatory example. Imagine that, after a few cases of a disease have been reported, we had developed a mathematical model to predict its spread. Suppose also that, in order to formulate this model, we had adopted a standard ADN with time-invariant activity rates, thereby neglecting any self-excitement effect. As a consequence, we would overestimate the epidemic threshold, and consequently underestimate the danger of the outbreak, with potential catastrophic consequences for the whole population. [Figure 5](#) illustrates this hypothetical scenario. The simulation of the SIS

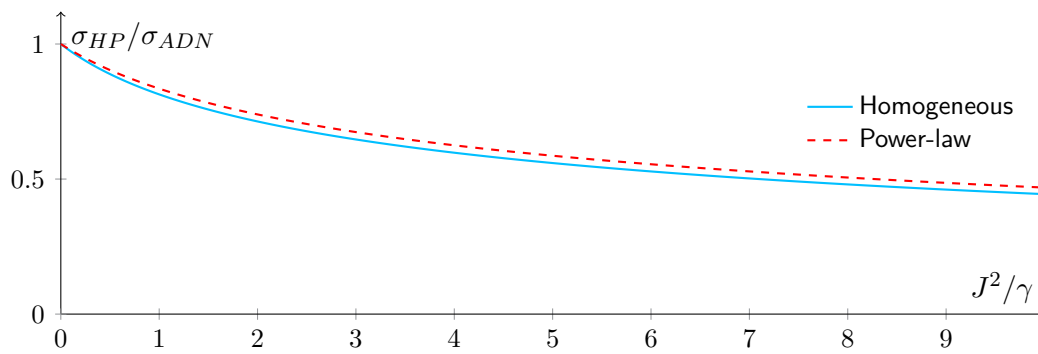


Figure 4. Ratio between the epidemic thresholds for an SIS model on an ADN+HP and on the corresponding ADN with time-invariant rates for increasing values of J^2/γ and different background activity rates: homogeneous with $\hat{a} = 0.225$ (light blue solid), and power-law distributed with exponent 2.09 and lower cut-off 0.15 (red dashed).

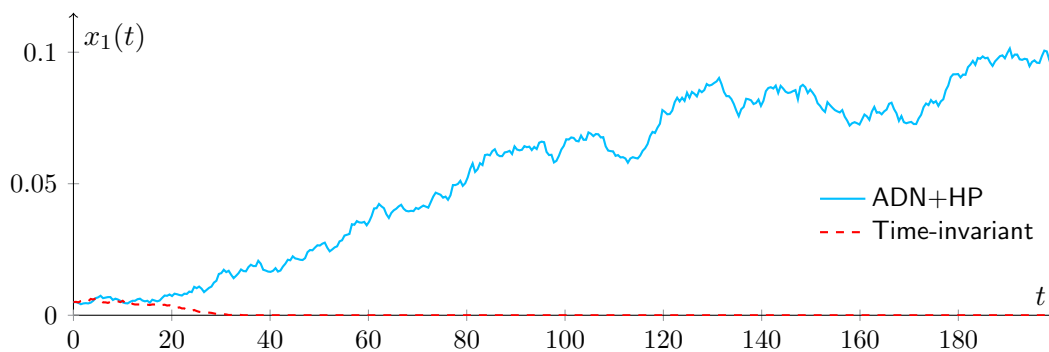


Figure 5. Sample paths of an SIS model (fraction of infected individuals) on an ADN+HP (light blue solid) and the corresponding ADN with time-invariant activity rates (red dashed) with homogeneous background activity rates $\hat{a} = 0.225$. Model parameters are $n = 10,000$, $\lambda = 0.43$, $\mu = 0.4$, $J = 0.4$, $\gamma = 0.8$, and the initial fraction of infected individuals $x_1(0) = 0.005$. The ADN with time-invariant activity rates is in the fast extinction regime, since $\lambda/\mu < \sigma \approx 1.1111$, while the ADN+HP is the endemic regime, since $\lambda/\mu > \sigma_{HP} \approx 1.1054$ (computed according to [Theorem 4.2](#)).

model on a standard ADN (blue curve) suggests a fast extinction of the disease (being the parameters below the epidemic threshold σ), while the one performed with self-excitement yields to the inception of an outbreak.

5. Numerical simulations. Here, we deepen our analysis of ADNs+HP through Monte Carlo numerical simulations, toward an improved understanding of the effects of self-excitation. The simulation of Hawkes processes is performed using the algorithm proposed in [18], whereas the continuous-time ADNs (for both the simulated models) are generated using a Gillespie algorithm [26]. Unless otherwise specified, the parameters used in epidemic models are those estimated for the real-world case study of an influenza outbreak in [89].

Our numerical computations pursue three objectives. First, we investigate the effect of heterogeneity and noise in the two parameters J and γ . Then, we strengthen the analysis of the SIS model by estimating the evolution of the epidemic prevalence through Monte Carlo

simulations and comparing it with the one without self-excitement. Finally, we discuss the effect of immunization combined with self-excitement by analyzing a Susceptible–Infected–Recovered (SIR) model [11].

5.1. Effect of heterogeneity and noise in the parameters. In subsection 4.1, we have analytically studied the effect of self-excitement on the activity rate distribution under the assumption that all the individuals in the population generate connections according to independent Hawkes processes with the same parameters J and γ for each individual. Under this assumption, we have been able to prove that self-excitement leads to broad and more disperse activity rate distributions, with a consequent increase of the network vulnerability to epidemic inception. We extend this analysis through a numerical study of the effect of heterogeneity and noise in the individuals' parameters.

We set the parameters

$$(5.1a) \quad J_v = J + \xi_v, \quad \xi_v \sim \mathcal{N}(0, \sigma_{\mathcal{N}}^2), \quad v \in \mathcal{V};$$

$$(5.1b) \quad \gamma_v = \gamma + \eta_v, \quad \eta_v \sim \mathcal{N}(0, \sigma_{\mathcal{N}}^2), \quad v \in \mathcal{V},$$

where all the ξ_v 's and η_v 's, $v \in \mathcal{V}$, are independent and identically distributed Gaussian RVs with mean equal to 0 and variance to $\sigma_{\mathcal{N}}^2$. Then, we let the ADN+HP evolve and converge to its asymptotic distribution, which, in our setup, requires running the simulation until $t = 200$. From our simulation results, illustrated in Figure 6, we observe that heterogeneity in the individual parameters causes a further increase of all the examined quantities (mean, square mean, and coefficient of variation of the activity rate distribution), compared with the corresponding homogeneous case. In agreement with our expectations, for the homogeneous case, all these quantities are accurately predicted by our analytical results (the blue dotted lines) in Lemma 4.1.

By comparing the results in the three top panels (obtained for a homogeneous background distribution) with those in the bottom panels (obtained adopting a power-law background distribution) of Figure 6, it is evident that the effect of heterogeneity in the self-excitement mechanisms becomes less significant when the background activity rate distribution is heterogeneous. In fact, from Figure 6c, we observe that when the background activity is homogeneous, the dispersion of the activity rate distribution increases by more than 45%. By contrast, the dispersion increases by less than 20% when the background activity rates are power-law distributed. Hence, numerical results support the proposition that uniform values of J and γ in the population can still lead to heterogeneity at the population level, provided that the background activity rate distribution is selected as a heavy-tailed distribution, following [1].

5.2. Epidemic prevalence for the SIS model. While most of the results on the SIS model pertain to the computation of its epidemic threshold, the analysis and prediction of the transient evolution of the process when the disease is above the epidemic threshold and becomes endemic are still open problems, with significant applications in public health [14, 39]. Through Monte Carlo simulations, we seek to offer an improved understanding of the effect of self-excitement on the endemic state of the disease.

In Figure 7, we compare the epidemic prevalence of an SIS model on an ADN+HP and on the corresponding ADN with time-invariant activity rates. We identify two opposite behaviors

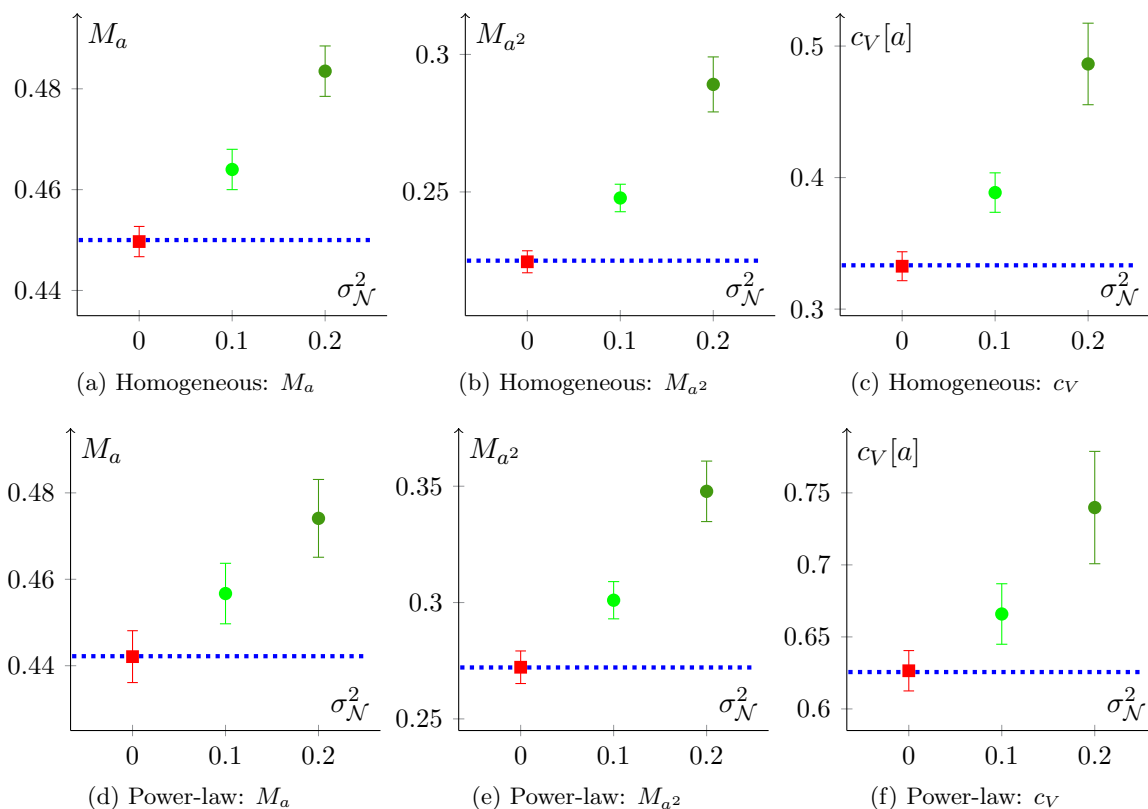


Figure 6. Estimated (a), (d) mean, (b), (e) mean square, and (c), (f) coefficient of variation of the activity rate distribution in asymptotic conditions for homogeneous values of J and γ (red squares) and for increasing heterogeneity (light and dark green circles, respectively). Model parameters are $n = 100,000$, $J = 0.1$, and $\gamma = 0.2$. An asymptotic condition is attained for $t = 200$. In (a)–(c), the background activity rates are homogeneous with $\hat{a} = 0.225$, and in (d)–(f) they are power-law distributed with exponent 2.09 and lower cut-off 0.15. Both the moment of the activity rate distribution and the coefficient of variation increase with the heterogeneity of the parameters J and γ . Results obtained over 200 independent Monte Carlo simulations. Markers are estimated values, while error bars represent the 95% confidence intervals for the estimated quantities.

in the transient phase, immediately after the inception of the disease, and at the endemic equilibrium, arising from a balance between new transmissions of the infection and recoveries. Specifically, we find that the presence of self-excitement tends to speed up the spread of the epidemic in the transient phase, consistently with the decreased epidemic threshold, but the fraction of infected individuals at the endemic equilibrium appears to be slightly reduced.

This phenomenon has an intuitive explanation: immediately after the inception of the epidemic outbreak, the first disease spreaders become active, tending to increase their activities and boosting the spread. After this first phase, the forgetting process tends to reduce the individuals’ activities, specifically of those who have been activated few times (and consequently are less likely to be infected), further decreasing the probability they can be infected.

5.3. Epidemic threshold for the SIR model. Finally, we discuss the combined effect of immunization and self-excitement by analyzing an SIR epidemic model [11] on an ADN+HP.

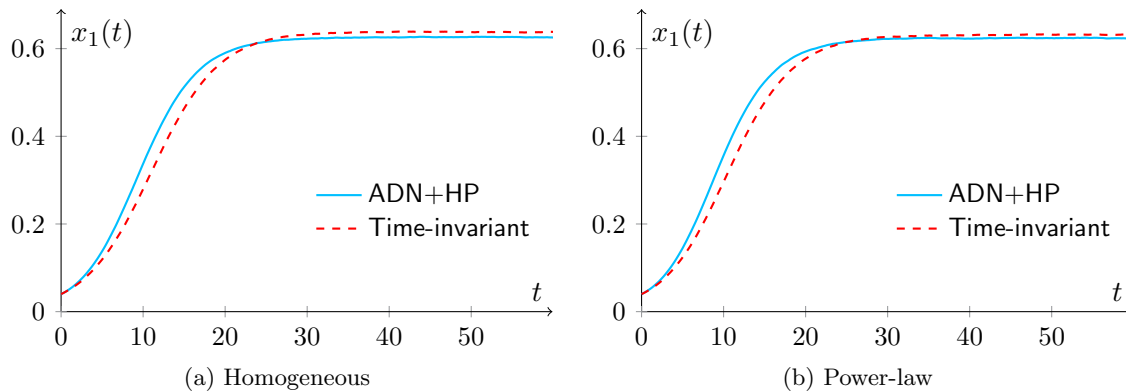


Figure 7. Monte Carlo estimation (over 500 independent simulations) of the epidemic prevalence for an SIS model on an ADN+HP (light blue solid) and on the corresponding ADN with time-invariant activity rates (red dashed) for different background activity rates: (a) homogeneous with $\hat{a} = 0.15$, and (b) power-law distributed with exponent 2.09 and lower cut-off 0.1. For both panels, the parameters are $\lambda = 0.43$, $\mu = 1/7$, $n = 2000$, $J = 0.4$, $\gamma = 0.8$, and the initial fraction of infected individuals $x_1(0) = 0.04$.

Similar to the SIS model, a variety of modeling choices are available when embedding an SIR epidemic model in a network. Here, we define an SIR model on an ADN+HP similar to the SIS model in [subsection 4.2](#), except for the recovery mechanism. When infected individuals recover, they become immune and cannot contract the epidemic again.

In [\[83\]](#), the characteristics of the epidemic spreading under SIS and SIR models have been numerically studied for the ADN model with the inclusion of memory processes in the link formation mechanism, as already discussed in the introduction. In these numerical simulations, an effect similar to that caused by self-excitement has been observed, whereby the epidemic threshold of the SIS model has been found to decrease due to memory on the link formation. On the other hand, when immunization is present, the epidemic threshold increases, making the network less prone to epidemic inception. Here, we observe a different behavior for the ADN+HP model.

In order to estimate the threshold for the SIR model, we adopt the method proposed in [\[59\]](#), where Monte Carlo simulations of the dynamics are performed for different choices of the ratio λ/μ . For the sake of simplicity, we fix $\lambda = 0.5$ and we let the parameter μ vary—the assumption $\lambda = 0.5$ does not reduce the generality of the SIR model, for which different values of λ can be interpreted as a time rescaling. Since the SIR model almost surely extinguishes in a finite time [\[20\]](#), we let the simulation evolve until no infected individual is present. Then, the threshold is estimated as the ratio λ/μ that maximizes the coefficient of variation of the fraction of individuals attained by the epidemic.

We determine that the combination of immunization with self-excitement has the opposite effect of its combination with memory in the link formation proposed in [\[83\]](#). Results in [Figure 8](#) suggest that immunization increases the network vulnerability, rather than hindering the inception of the disease spreading. In fact, while the threshold for the SIS model and the one for the SIR model coincide for a standard ADN model (the red dashed line and peak of the red curve in [Figure 8a](#), respectively) [\[90\]](#), the estimated epidemic threshold for the SIR

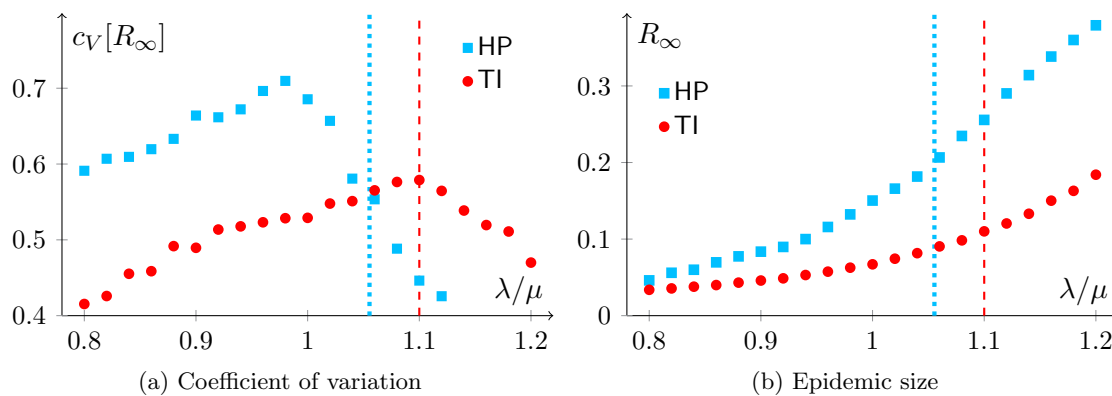


Figure 8. Monte Carlo estimation (over 200 independent simulations) of the epidemic threshold for an SIR model on an ADN+HP (light blue squares) and the corresponding ADN with time-invariant activity rates (red circles). In panel (a), the threshold is estimated by identifying the peak of the coefficient of variation $c_V[R_\infty]$. Vertical lines correspond to the analytical thresholds for the SIS model in the presence of self-excitement computed using *Theorem 4.2* (light blue dotted) and in the absence of it (red dashed). In panel (b), the average epidemic size (fraction of individuals reached by the epidemic) R_∞ on the two network models is compared. Simulation parameters are $n = 2,000$, $J = 0.4$, $\lambda = 0.5$, and $\gamma = 0.8$, the background activity rates are homogeneous with $\hat{a} = 0.225$, and the spreading process starts from a single infected node, randomly selected in the population.

model on an ADN+HP (peak of the light blue curve in [Figure 8a](#)) registers a larger shift than the threshold analytically computed for the SIS model (light blue dotted line). Finally, in [Figure 8b](#) we observe that, along with the decreased threshold, self-excitement leads to an increased size of the epidemic, measured as the fraction of individuals reached by the disease during the outbreak.

The increased vulnerability in the presence of immunization has the following explanation. Similar to the SIS model, immediately after an individual activates and contracts the disease, he/she increases its activity due to self-excitement, thereby boosting the spread in the transient phase. Then, in an SIS model, the forgetting process compensates for this increase, as can be seen when the disease becomes endemic from [Figure 7](#). On the contrary, in the SIR model the system evolution is limited to the transient phase, after which the disease-free equilibrium is reached [20]. Therefore, the presence of immunization tends to amplify the boost produced by self-excitement and to weaken the slow-down effect of the forgetting process. Besides applications in epidemiology, we believe that these observations could be of broad interest in opinion dynamics, e.g., to model the spread of information and hoaxes, for which self-excitement mechanisms might explain unexpected spreading [84].

6. Conclusion. In this paper, we have developed an analytically tractable model of time-varying networks that generalizes the paradigm of ADNs by including dynamics in the individuals’ social activity. These temporal variations are ruled by Hawkes processes, which only rely on two parameters that control a self-excitement mechanism and a forgetting process. Despite its simplicity, this model is able to reproduce the presence of phenomena that are often observed in empirical data, such as burstiness of human behaviors and proneness of the

events to cluster.

We have shown the possibility of analytically tackling this model by leveraging standard techniques used in networks science (i.e., mean-field theory and thermodynamic considerations) and methods from the field of SDEs (i.e., Ito's lemma and Dynkin's formula). Specifically, under some reasonable assumptions, we have been able to analyze the long-run behavior of the individual's activity and to estimate the epidemic threshold of an SIS model.

From these results and Monte Carlo numerical simulations, we have shown that the main effect of self-excitement is to increase the variability of the individual's social activity. In turn, in our settings, this decreases the epidemic threshold of the system, thereby increasing the network vulnerability to epidemic outbreaks, both in the presence of reinfection mechanisms (SIS model) and with immunization dynamics (SIR model). These claims could be consolidated into a main conclusive message: neglecting self-excitement might have dramatic consequences for the society, leading to the underestimation of the risk of an epidemic outbreak.

Several future research lines arise from the development of this model and the analysis we have performed. First, further efforts are required to deepen our analytical investigation and understand, e.g., how the falloff of the tail distribution depends on the background activity and on the model parameters. We also seek to extend the analytical approach to study the effect of heterogeneous self-excitement mechanisms in the population, which in this paper has been tackled only numerically. Second, in [90], a framework based on the discretization of the activity rate distribution has been established to analytically study the transient evolution of epidemic processes on ADNs. We believe that this framework could be similarly extended to ADNs+HP by dividing nodes into classes of background activity rates. Third, our model is very flexible and allows for the inclusion of real-world phenomena, such as memory processes and communities in the connection pattern, behavioral changes due to the individuals' state, spatial locality, and communication delays. The analysis of their effect and the study of different network dynamics including synchronization and state-dependent spreading processes [77, 78] will be part of our future work. For example, when modeling the outbreak of an epidemic disease, one should also consider that infected individuals tend to decrease their activity, after the disease becomes symptomatic. The contrasting effects of self-excitement when the disease is asymptomatic and the following activity reduction due to the illness will be analyzed in our future research and might lead to interesting insights into the epidemic process. Fourth, the analytical treatment in this paper is limited to the thermodynamic limit. In our future research, we will seek to extend our theory to networks of finite size, by leveraging techniques from the stochastic Lyapunov theory. Finally, the identification from empirical data of the two new model parameters, i.e., the jump J and the forgetting rate γ , is yet to be discussed. Consequently, the transition of our model to real-world scenarios will be the object of future research.

Pursuing these lines of inquiry would lead to a definition of a model of temporal networks with the capability of describing evolving networks with a strong potential for explaining and predicting critical real-world phenomena.

Acknowledgment. The authors would like to thank Matthieu Nadini for productive discussions about the mathematical model and the methods for numerical simulations.

REFERENCES

- [1] W. AIELLO, F. CHUNG, AND L. LU, *A random graph model for power law graphs*, *Exp. Math.*, 10 (2001), pp. 53–66.
- [2] L. ALESSANDRETTI, K. SUN, A. BARONCHELLI, AND N. PERRA, *Random walks on activity-driven networks with attractiveness*, *Phys. Rev. E* (3), 95 (2017), 052318, <https://doi.org/10.1103/PhysRevE.95.052318>.
- [3] R. A. S. ALVES, R. M. ASSUNCAO, AND P. O. S. VAZ DE MELO, *Burstiness scale: A parsimonious model for characterizing random series of events*, in *Proceedings of the 22nd ACM SIGKDD International Conference on Knowledge Discovery and Data Mining, KDD '16*, 2016, pp. 1405–1414, <https://doi.org/10.1145/2939672.2939852>.
- [4] N. BACAËR AND S. GUERNAOUI, *The epidemic threshold of vector-borne diseases with seasonality*, *J. Math. Biol.*, 53 (2006), pp. 421–436, <https://doi.org/10.1007/s00285-006-0015-0>.
- [5] E. BACRY, I. MASTROMATTEO, AND J.-F. MUZY, *Hawkes processes in finance*, *Market Microstructure and Liquidity*, 01 (2015), 1550005, <https://doi.org/10.1142/S2382626615500057>.
- [6] N. T. J. BAILEY, *The Mathematical Theory of Infectious Diseases and its Applications*, 2nd ed., Griffin, London, 1975.
- [7] N. T. J. BAILEY, *The Elements of Stochastic Processes with Applications to the Natural Sciences*, John Wiley & Sons, New York, 1990.
- [8] A.-L. BARABÁSI, *The origin of bursts and heavy tails in human dynamics*, *Nature*, 435 (2005), pp. 207–211, <https://doi.org/10.1038/nature03459>.
- [9] C. BLUNDELL, J. M. BECK, AND K. A. HELLER, *Modelling reciprocating relationships with Hawkes processes*, in *Advances in Neural Information Processing Systems 25 (NIPS 2012)*, F. Pereira, C. J. C. Burges, L. Bottou, and K. Q. Weinberger, eds., Curran Associates, Inc., 2012, pp. 2600–2608.
- [10] M. BOGUÑÁ, R. PASTOR-SATORRAS, AND A. VESPIGNANI, *Absence of epidemic threshold in scale-free networks with degree correlations*, *Phys. Rev. Lett.*, 90 (2003), 028701, <https://doi.org/10.1103/PhysRevLett.90.028701>.
- [11] F. BRAUER AND C. CASTILLO-CHAVEZ, *Mathematical Models in Population Biology and Epidemiology*, 2nd ed., Springer, New York, 2012, <https://doi.org/10.1007/978-1-4614-1686-9>.
- [12] P. BRÉMAUD AND L. MASSOULIÉ, *Hawkes branching point processes without ancestors*, *J. Appl. Probab.*, 38 (2001), pp. 122–135, <https://doi.org/10.1239/jap/996986648>.
- [13] C. G. CASSANDRA AND S. LAFORTUNE, *Introduction to Discrete Event Systems*, 2nd ed., Springer, New York, 2008, <https://doi.org/10.1007/978-0-387-68612-7>.
- [14] G. CHOWELL, L. SATTENSPIEL, S. BANSAL, AND C. VIBOUD, *Mathematical models to characterize early epidemic growth: A review*, *Phys. Life Rev.*, 18 (2016), pp. 66–97, <https://doi.org/10.1016/j.plrev.2016.07.005>.
- [15] K. L. CHUNG, *A Course in Probability Theory, Revised Edition*, 3rd ed., Academic Press, San Diego, CA, 2001.
- [16] J. DA FONSECA AND R. ZAAOUR, *Hawkes process: Fast calibration, application to trade clustering, and diffusive limit*, *J. Futures Markets*, 34 (2014), pp. 548–579, <https://doi.org/10.1002/fut.21644>.
- [17] A. DASSIOS AND H. ZHAO, *A dynamic contagion process*, *Adv. Appl. Probab.*, 43 (2011), pp. 814–846, <https://doi.org/10.1239/aap/1316792671>.
- [18] A. DASSIOS AND H. ZHAO, *Exact simulation of Hawkes process with exponentially decaying intensity*, *Electron. Commun. Probab.*, 18 (2013), pp. 62–74, <https://doi.org/10.1214/ECP.v18-2717>.
- [19] A. DAW AND J. PENDER, *Queues Driven by Hawkes Processes*, preprint, <https://arxiv.org/abs/1707.05143v3>, 2017.
- [20] N. T. DIEU, D. H. NGUYEN, N. H. DU, AND G. YIN, *Classification of asymptotic behavior in a stochastic SIR model*, *SIAM J. Appl. Dyn. Syst.*, 15 (2016), pp. 1062–1084, <https://doi.org/10.1137/15M1043315>.
- [21] M. DRAIEF AND L. MASSOULIÉ, *Epidemics and Rumours in Complex Networks*, Cambridge University Press, Cambridge, UK, 2009, <https://doi.org/10.1017/CBO9780511806018>.
- [22] V. M. EGUÍLIZ AND K. KLEMM, *Epidemic threshold in structured scale-free networks*, *Phys. Rev. Lett.*, 89 (2002), 108701, <https://doi.org/10.1103/PhysRevLett.89.108701>.
- [23] F. FAGNANI AND L. ZINO, *Diffusion of innovation in large scale graphs*, *IEEE Trans. Netw. Sci. Eng.*, 4 (2017), pp. 100–111, <https://doi.org/10.1109/TNSE.2017.2678202>.

- [24] B. K. FOSDICK, D. B. LARREMORE, J. NISHIMURA, AND J. UGANDER, *Configuring random graph models with fixed degree sequences*, SIAM Rev., 60 (2018), pp. 315–355, <https://doi.org/10.1137/16M1087175>.
- [25] E. W. FOX, M. B. SHORT, F. P. SCHOENBERG, K. D. CORONGES, AND A. L. BERTOZZI, *Modeling e-mail networks and inferring leadership using self-exciting point processes*, J. Amer. Statist. Assoc., 111 (2016), pp. 564–584, <https://doi.org/10.1080/01621459.2015.1135802>.
- [26] D. T. GILLESPIE, *A general method for numerically simulating the stochastic time evolution of coupled chemical reactions*, J. Comput. Phys., 22 (1976), pp. 403–434, [https://doi.org/10.1016/0021-9991\(76\)90041-3](https://doi.org/10.1016/0021-9991(76)90041-3).
- [27] K.-I. GOH AND A.-L. BARABÁSI, *Burstiness and memory in complex systems*, Europhys. Lett., 81 (2008), 48002, <https://doi.org/10.1209/0295-5075/81/48002>.
- [28] A. GRAY, D. GREENHALGH, L. HU, X. MAO, AND J. PAN, *A stochastic differential equation SIS epidemic model*, SIAM J. Appl. Math., 71 (2011), pp. 876–902, <https://doi.org/10.1137/10081856X>.
- [29] T. GROSS, C. J. D. D’LIMA, AND B. BLASIUS, *Epidemic dynamics on an adaptive network*, Phys. Rev. Lett., 96 (2006), 208701, <https://doi.org/10.1103/PhysRevLett.96.208701>.
- [30] D. HAN, M. SUN, AND D. LI, *Epidemic process on activity-driven modular networks*, Phys. A, 432 (2015), pp. 354–362, <https://doi.org/10.1016/j.physa.2015.03.062>.
- [31] A. G. HAWKES, *Spectra of some self-exciting and mutually exciting point processes*, Biometrika, 58 (1971), pp. 83–90, <https://doi.org/10.1093/biomet/58.1.83>.
- [32] A. G. HAWKES, *Hawkes processes and their applications to finance: A review*, Quant. Finance, 18 (2018), pp. 193–198, <https://doi.org/10.1080/14697688.2017.1403131>.
- [33] J. HINDES, I. B. SCHWARTZ, AND L. B. SHAW, *Enhancement of large fluctuations to extinction in adaptive networks*, Phys. Rev. E (3), 97 (2018), 012308, <https://doi.org/10.1103/PhysRevE.97.012308>.
- [34] T. HOFFMANN, M. A. PORTER, AND R. LAMBIOTTE, *Generalized master equations for non-Poisson dynamics on networks*, Phys. Rev. E (3), 86 (2012), 046102, <https://doi.org/10.1103/PhysRevE.86.046102>.
- [35] P. HOLME, *Modern temporal network theory: A colloquium*, Eur. Phys. J. B, 88 (2015), 234, <https://doi.org/10.1140/epjb/e2015-60657-4>.
- [36] P. HOLME AND J. SARAMÄKI, *Temporal networks*, Phys. Rep., 519 (2012), pp. 97–125, <https://doi.org/10.1016/j.physrep.2012.03.001>.
- [37] D. X. HORVÁTH AND J. KERTÉSZ, *Spreading dynamics on networks: The role of burstiness, topology and non-stationarity*, New J. Phys., 16 (2014), 073037, <https://doi.org/10.1088/1367-2630/16/7/073037>.
- [38] C. HUEPE, G. ZSCHALER, A.-L. DO, AND T. GROSS, *Adaptive-network models of swarm dynamics*, New J. Phys., 13 (2011), 073022, <https://doi.org/10.1088/1367-2630/13/7/073022>.
- [39] A. HUPPERT AND G. KATRIEL, *Mathematical modelling and prediction in infectious disease epidemiology*, Clin. Microbiol. Infect., 19 (2013), pp. 999–1005, <https://doi.org/10.1111/1469-0691.12308>.
- [40] H. JIANG AND C. DOVROLIS, *Why is the internet traffic bursty in short time scales?*, SIGMETRICS Perf. Eval. Rev., 33 (2005), pp. 241–252, <https://doi.org/10.1145/1071690.1064240>.
- [41] M. KARSAI, N. PERRA, AND A. VESPIGNANI, *Time varying networks and the weakness of strong ties*, Sci. Rep., 4 (2014), 4001, <https://doi.org/10.1038/srep04001>.
- [42] M. KIVELÄ AND M. A. PORTER, *Estimating interevent time distributions from finite observation periods in communication networks*, Phys. Rev. E (3), 92 (2015), 052813, <https://doi.org/10.1103/PhysRevE.92.052813>.
- [43] V. S. KULKARNI, *Temporal evolution of social innovation: What matters?*, SIAM J. Appl. Dyn. Syst., 15 (2016), pp. 1485–1500, <https://doi.org/10.1137/15M1040797>.
- [44] T. G. KURTZ, *Solutions of ordinary differential equations as limits of pure jump Markov processes*, J. Appl. Probab., 7 (1970), pp. 49–58, <https://doi.org/10.2307/3212147>.
- [45] T. G. KURTZ, *Limit theorems for sequences of jump Markov processes approximating ordinary differential processes*, J. Appl. Probab., 8 (1971), pp. 344–356, <https://doi.org/10.2307/3211904>.
- [46] R. LAMBIOTTE, L. TABOURIER, AND J.-C. DELVENNE, *Burstiness and spreading on temporal networks*, Eur. Phys. J. B, 86 (2013), 320, <https://doi.org/10.1140/epjb/e2013-40456-9>.
- [47] P. J. LAUB, T. TAIMRE, AND P. K. POLLETT, *Hawkes Processes*, preprint, <https://arxiv.org/abs/1507.02822>, 2015.
- [48] Y. LEI, X. JIANG, Q. GUO, Y. MA, M. LI, AND Z. ZHENG, *Contagion processes on the static and activity-driven coupling networks*, Phys. Rev. E (3), 93 (2016), 032308, <https://doi.org/10.1103/PhysRevE.93.032308>.

- [49] E. LEWIS, G. MOHLER, P. J. BRANTINGHAM, AND A. L. BERTOZZI, *Self-exciting point process models of civilian deaths in Iraq*, *Secur. J.*, 25 (2012), pp. 244–264, <https://doi.org/10.1057/sj.2011.21>.
- [50] D. LI, D. HAN, J. MA, M. SUN, L. TIAN, T. KHOUW, AND H. E. STANLEY, *Opinion dynamics in activity-driven networks*, *Europhys. Lett.*, 120 (2017), 28002, <https://doi.org/10.1209/0295-5075/120/28002>.
- [51] C. LIU, L.-X. ZHOU, C.-J. FAN, L.-A. HUO, AND Z.-W. TIAN, *Activity of nodes reshapes the critical threshold of spreading dynamics in complex networks*, *Phys. A*, 432 (2015), pp. 269–278, <https://doi.org/10.1016/j.physa.2015.03.054>.
- [52] S. LIU, N. PERRA, M. KARSAI, AND A. VESPIGNANI, *Controlling contagion processes in activity driven networks*, *Phys. Rev. Lett.*, 112 (2014), 118702, <https://doi.org/10.1103/PhysRevLett.112.118702>.
- [53] A. LYNCH, *Thought Contagion. How Belief Spreads Through Society: The New Science of Memes*, Basic Books, New York, 1996.
- [54] R. D. MALMGREN, D. B. STOUFFER, A. E. MOTTER, AND L. A. N. AMARAL, *A Poissonian explanation for heavy tails in e-mail communication*, *Proc. Natl. Acad. Sci. USA*, 105 (2008), pp. 18153–18158, <https://doi.org/10.1073/pnas.0800332105>.
- [55] D. MARSAN AND O. LENGLINÉ, *Extending earthquakes' reach through cascading*, *Science*, 319 (2008), pp. 1076–1079, <https://doi.org/10.1126/science.1148783>.
- [56] N. MASUDA, T. TAKAGUCHI, N. SATO, AND K. YANO, *Self-exciting point process modeling of conversation event sequences*, in *Temporal Networks. Understanding Complex Systems*, Springer, Berlin, Heidelberg, 2013, pp. 245–264, https://doi.org/10.1007/978-3-642-36461-7_12.
- [57] P. V. MIEGHEM, J. OMIC, AND R. KOOLJ, *Virus spread in networks*, *IEEE/ACM Trans. Netw.*, 17 (2009), pp. 1–14, <https://doi.org/10.1109/TNET.2008.925623>.
- [58] G. O. MOHLER, M. B. SHORT, P. J. BRANTINGHAM, F. P. SCHOENBERG, AND G. E. TITA, *Self-exciting point process modeling of crime*, *J. Amer. Statist. Assoc.*, 106 (2011), pp. 100–108, <https://doi.org/10.1198/jasa.2011.ap09546>.
- [59] A. MOINET, R. PASTOR-SATORRAS, AND A. BARRAT, *Effect of risk perception on epidemic spreading in temporal networks*, *Phys. Rev. E* (3), 97 (2018), 012313, <https://doi.org/10.1103/PhysRevE.97.012313>.
- [60] S. MORITA, *Six susceptible-infected-susceptible models on scale-free networks*, *Sci. Rep.*, 6 (2016), 22506, <https://doi.org/10.1038/srep22506>.
- [61] V. MWAFFO, R. P. ANDERSON, S. BUTAIL, AND M. PORFIRI, *A jump persistent turning walker to model zebrafish locomotion*, *J. Royal Soc. Interface*, 12 (2015), 20140884, <https://doi.org/10.1098/rsif.2014.0884>.
- [62] M. NADINI, K. SUN, E. UBALDI, M. STARNINI, A. RIZZO, AND N. PERRA, *Epidemic spreading in modular time-varying networks*, *Sci. Rep.*, 8 (2018), 2352, <https://doi.org/10.1038/s41598-018-20908-x>.
- [63] B. ØKSENDAL, *Stochastic Differential Equations: An Introduction with Applications*, 6th ed., Springer, Berlin, 2003, <https://doi.org/10.1007/978-3-642-14394-6>.
- [64] V. PARETO, *Cours d'Economie Politique*, F. Rouge, Lausanne, Switzerland, 1896.
- [65] R. PARSHANI, S. CARMI, AND S. HAVLIN, *Epidemic threshold for the susceptible-infectious-susceptible model on random networks*, *Phys. Rev. Lett.*, 104 (2010), 258701, <https://doi.org/10.1103/PhysRevLett.104.258701>.
- [66] R. PASTOR-SATORRAS, C. CASTELLANO, P. VAN MIEGHEM, AND A. VESPIGNANI, *Epidemic processes in complex networks*, *Rev. Modern Phys.*, 87 (2015), pp. 925–979, <https://doi.org/10.1103/RevModPhys.87.925>.
- [67] R. PASTOR-SATORRAS AND A. VESPIGNANI, *Epidemic spreading in scale-free networks*, *Phys. Rev. Lett.*, 86 (2001), 3200, <https://doi.org/10.1103/PhysRevLett.86.3200>.
- [68] V. PAXSON AND S. FLOYD, *Wide area traffic: The failure of Poisson modeling*, *IEEE/ACM Trans. Netw.*, 3 (1995), pp. 226–244, <https://doi.org/10.1109/90.392383>.
- [69] N. PERRA, B. GONÇALVES, R. PASTOR-SATORRAS, AND A. VESPIGNANI, *Activity driven modeling of time varying networks*, *Sci. Rep.*, 2 (2012), 469, <https://doi.org/10.1038/srep00469>.
- [70] G. PETRI AND A. BARRAT, *Simplicial Activity Driven Model*, preprint, <https://arxiv.org/abs/1805.06740v2>, 2018.
- [71] I. POZZANA, K. SUN, AND N. PERRA, *Epidemic spreading on activity-driven networks with attractiveness*, *Phys. Rev. E* (3), 96 (2017), 042310, <https://doi.org/10.1103/PhysRevE.96.042310>.

- [72] B. RIBEIRO, N. PERRA, AND A. BARONCHELLI, *Quantifying the effect of temporal resolution on time-varying networks*, *Sci. Rep.*, 3 (2013), 3006, <https://doi.org/10.1038/srep03006>.
- [73] M.-A. RIZOIU, L. XIE, S. SANNER, M. CEBRIAN, H. YU, AND P. VAN HENTENRYCK, *Expecting to be HIP: Hawkes intensity processes for social media popularity*, in Proceedings of the 26th International Conference on World Wide Web, WWW '17, International World Wide Web Conferences Steering Committee, 2017, pp. 735–744, <https://doi.org/10.1145/3038912.3052650>.
- [74] A. RIZZO, M. FRASCA, AND M. PORFIRI, *Effect of individual behavior on epidemic spreading in activity-driven networks*, *Phys. Rev. E* (3), 90 (2014), 042801, <https://doi.org/10.1103/PhysRevE.90.042801>.
- [75] A. RIZZO, B. PEDALINO, AND M. PORFIRI, *A network model for Ebola spreading*, *J. Theoret. Biol.*, 394 (2016), pp. 212–222, <https://doi.org/10.1016/j.jtbi.2016.01.015>.
- [76] A. RIZZO AND M. PORFIRI, *Innovation diffusion on time-varying activity driven networks*, *Eur. Phys. J. B*, 89 (2016), 20, <https://doi.org/10.1140/epjb/e2015-60933-3>.
- [77] G. RUSSO AND R. SHORTEN, *On common noise-induced synchronization in complex networks with state-dependent noise diffusion processes*, *Phys. D*, 369 (2018), pp. 47–54, <https://doi.org/10.1016/j.physd.2018.01.003>.
- [78] G. RUSSO, F. WIRTH, AND R. SHORTEN, *On synchronization in continuous-time networks of nonlinear nodes with state dependent and degenerate noise diffusion*, *IEEE Trans. Automat. Control*, (2018), <https://doi.org/10.1109/TAC.2018.2829462>.
- [79] L. B. SHAW AND I. B. SCHWARTZ, *Fluctuating epidemics on adaptive networks*, *Phys. Rev. E* (3), 77 (2008), 066101, <https://doi.org/10.1103/PhysRevE.77.066101>.
- [80] R. SIPAHI, F. M. ATAY, AND S.-I. NICULESCU, *Stability of traffic flow behavior with distributed delays modeling the memory effects of the drivers*, *SIAM J. Appl. Math.*, 68 (2007), pp. 738–759, <https://doi.org/10.1137/060673813>.
- [81] M. STARNINI AND R. PASTOR-SATORRAS, *Temporal percolation in activity-driven networks*, *Phys. Rev. E* (3), 89 (2014), 032807, <https://doi.org/10.1103/PhysRevE.89.032807>.
- [82] A. STOMAKHIN, M. B. SHORT, AND A. L. BERTOZZI, *Reconstruction of missing data in social networks based on temporal patterns of interactions*, *Inverse Problems*, 27 (2011), 115013, <https://doi.org/10.1088/0266-5611/27/11/115013>.
- [83] K. SUN, A. BARONCHELLI, AND N. PERRA, *Contrasting effects of strong ties on SIR and SIS processes in temporal networks*, *Eur. Phys. J. B*, 88 (2015), 326, <https://doi.org/10.1140/epjb/e2015-60568-4>.
- [84] M. TAMBUSCIO, G. RUFFO, A. FLAMMINI, AND F. MENCZER, *Fact-checking effect on viral hoaxes*, in Proceedings of the 24th International ACM Conference on World Wide Web (WWW '15 Companion), 2015, pp. 977–982, <https://doi.org/10.1145/2740908.2742572>.
- [85] E. UBALDI, A. VEZZANI, M. KARSAI, N. PERRA, AND R. BURIONI, *Burstiness and tie activation strategies in time-varying social networks*, *Sci. Rep.*, 7 (2017), 46225, <https://doi.org/10.1038/srep46225>.
- [86] E. VOLZ AND L. A. MEYERS, *Epidemic thresholds in dynamic contact networks*, *J. Royal Soc. Interface*, 6 (2009), pp. 233–241, <https://doi.org/10.1098/rsif.2008.0218>.
- [87] Q. ZHAO, M. A. ERDOGDU, H. Y. HE, A. RAJARAMAN, AND J. LESKOVEC, *SEISMIC: A self-exciting point process model for predicting tweet popularity*, in Proceedings of the 21th ACM SIGKDD International Conference on Knowledge Discovery and Data Mining, KDD '15, 2015, pp. 1513–1522, <https://doi.org/10.1145/2783258.2783401>.
- [88] L. ZINO, G. COMO, AND F. FAGNANI, *Fast diffusion of a mutant in controlled evolutionary dynamics*, in Proceedings of the 20th IFAC World Congress, IFAC-PapersOnLine, 50 (2017), pp. 11908–11913, <https://doi.org/10.1016/j.ifacol.2017.08.1429>.
- [89] L. ZINO, A. RIZZO, AND M. PORFIRI, *Continuous-time discrete-distribution theory for activity-driven networks*, *Phys. Rev. Lett.*, 117 (2016), 228302, <https://doi.org/10.1103/PhysRevLett.117.228302>.
- [90] L. ZINO, A. RIZZO, AND M. PORFIRI, *An analytical framework for the study of epidemic models on activity driven networks*, *J. Complex Netw.*, 5 (2017), pp. 924–952, <https://doi.org/10.1093/comnet/cnx056>.
- [91] Y. ZOU, W. DENG, W. LI, AND X. CAI, *A study of epidemic spreading on activity-driven networks*, *Internat. J. Modern Phys. C*, 27 (2016), 1650090, <https://doi.org/10.1142/S012918311650090X>.